PHYSICAL REVIEW A **88**, 041805(R) (2013)

Remotely pumped stimulated emission at 337 nm in atmospheric nitrogen

Daniil Kartashov,[1] Skirmantas Ališauskas,[1] Andrius Baltuška,[1] Andreas Schmitt-Sody,[2] William Roach,[2] and Pavel Polynkin[3,*]

[1]*Photonics Institute, Vienna University of Technology, A-1040 Vienna, Austria*

[2]*Air Force Research Laboratory, Kirtland Air Force Base, Albuquerque, New Mexico 87116, USA*

[3]*College of Optical Sciences, The University of Arizona, Tucson, Arizona 85721, USA*

(Received 19 July 2013; published 30 October 2013)

We report the observation of forward-propagating UV stimulated emission in atmospheric nitrogen pumped, at a standoff distance of 2.6 m, by an energetic laser pulse at a wavelength of 1053 nm and with the duration in the picosecond range. The generated optical gain at 337 nm is seeded by third harmonic of the pump beam. This demonstration is an important step towards the development of techniques for standoff optical sensing in the atmosphere.

DOI: 10.1103/PhysRevA.88.041805 PACS number(s): 42.55.Lt, 42.65.Jx, 42.72.Bj

The realization of remotely pumped laserlike sources in air is an enabling step towards the development of various standoff sensing schemes [1,2]. In recent demonstrations [3,4], deep-UV laser pulses with a wavelength of 226 nm have been used to simultaneously dissociate molecular oxygen in air and to pump, via a two-photon process, a transient backward-propagating laser emission at a 845-nm wavelength. High absorption and scattering losses for deep-UV pump light in atmosphere impose a limitation on the range at which this approach can be implemented.

Another major constituent of air, besides oxygen, is nitrogen. An intense research effort is currently under way that targets the development of lasing schemes in various forms of this element. It has been suggested that dilute plasma filaments [5–7], which are produced through self-focusing of ultraintense femtosecond laser pulses in air, can emit directional laserlike radiation on the 357- and 391-nm electronic transitions of neutral and singly ionized nitrogen molecules, respectively. Detection of such emission in the backward direction has been reported [8]. The emission was very weak. It was only detectable with a photomultiplier and the measurement results were specified on an arbitrary unit scale.

More recently, the observation of forward-propagating emission on various UV lines of singly ionized nitrogen molecule has been reported, under the conditions of pumping by tightly focused, tunable mid-IR femtosecond laser pulses [9]. The emission on a particular transition in molecular nitrogen ions was observed when the wavelength of the fifth harmonic of the tunable pump light fell in the spectral vicinity of that transition, suggesting that the emission process was seeded by the fifth harmonic of the pump beam. The extension of these experiments to the cases of various gases mixed with nitrogen has been recently reported [10]. As in [8], the energy of the emission was too low to be measurable on the absolute unit scale.

It is worthwhile to mention that the generation of impulsive laser emission on several UV lines of nitrogen in air was reported more than 20 years ago using pumping by high-power microwaves [11]. The emission was demonstrated inside a microwave waveguide, in both forward and backward directions relative to the pumping microwave beam. Extending the range of the microwave pumping-based approach to significant standoff distances is not possible because of the rapid diffractive divergence of microwave beams.

In this paper, we report the demonstration of a transient UV nitrogen lasing at 337 nm at a standoff distance of 2.6 m. Our lasing scheme utilizes pumping by energetic infrared laser pulses with the duration in the picosecond range. It is found to be equally effective in pure nitrogen and in atmospheric air. The generated 337-nm emission is sufficiently strong to be measurable on the absolute unit scale.

The experiments reported here have been conducted using the Comet laser system, which is a part of the Jupiter Laser Facility at the Lawrence Livermore National Laboratory [12]. The Comet is a Nd glass-based chirped-pulse amplification chain that generates laser pulses at 1053-nm wavelength, with up to 10 J of energy per pulse. The transform-limited output pulse duration is 0.5 ps. The pulses are generated at a rate of about one pulse in 5 min.

The experimental setup is shown schematically in Fig. 1. The collimated beam generated by the Comet laser has a diameter of 90 mm. The beam passes through a 10-mm-thick fused silica exit window of the vacuum compressor chamber of the laser into an approximately 5-m-long gas cell filled with either air or pure nitrogen at atmospheric pressure. The laser beam is focused by a meniscus lens with a focal length of 2.6 m. The thickness of the lens at its center is about 3 mm. The pulse energy is varied by changing the pump level in the final amplifier stage. The pulse duration is controlled through tuning the pulse stretcher in the laser system.

The focused laser beam creates a plasma channel inside the gas chamber, near the focal plane of the meniscus lens. The length of the plasma channel is estimated by analyzing photographic side images of plasma fluorescence and is found to be about 10 cm. The transverse intensity profile in the interaction zone is inferred from single-shot burn patterns produced by the laser beam on an uncoated glass surface placed in the center of the Rayleigh zone of the beam. The profile is found to be round and, for a 10-J 10-ps pulse, about 5 mm in diameter. We were not able to determine from the appearance of the burn patterns whether the transverse intensity profile of the beam in the interaction zone was uniform or fragmented into individual filaments.

*ppolynkin@optics.arizona.edu

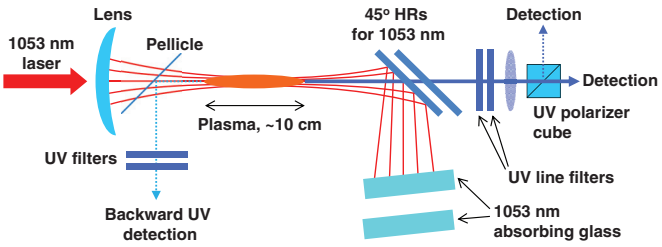

FIG. 1. (Color online) Schematic of the experimental setup.

For the detection of the generated UV light in the forward direction, the beam is reflected by two consecutive 45° dichroic mirrors that are highly reflective for the pump light and transmissive for the UV. The reflected pump is subsequently absorbed in two 30-mm-thick colored-glass plates. The left-over pump light transmitted through the dichroic mirrors is blocked by several interference filters that reject the pump and transmit various UV spectral lines of interest. The transmitted UV light is separated into two polarization components, one of which is parallel and the other perpendicular to the polarization of the pump beam, using a polarizer cube. The UV spectra of both polarizations are recorded by placing entrance slits of compact spectrometers directly into the beam paths, after the polarization separator.

It is known that for the case of a UV nitrogen laser pumped by electrical discharge, the addition of even a low percent of oxygen to the gas strongly inhibits the lasing. This effect results from the efficient quenching of the upper and the lower lasing levels of nitrogen through collisions with oxygen molecules. The corresponding reaction leads to the deexcitation of the nitrogen molecule into the ground state and dissociation of oxygen and, in ambient air, occurs on the nanosecond time scale [13]. As we will show below, the nitrogen emission in our experiment is seeded by the third harmonic of the pump beam and therefore occurs on the time scale defined by the duration of the pump pulse, which is of the order of 10 ps. That is much faster than the collisional quenching reaction. Accordingly, the experimental data obtained in pure nitrogen gas were essentially identical to those obtained in ambient air, which is important for practical applications of our results. All the data shown below were obtained in ambient air.

The examination of the UV part of the emission spectrum in the forward direction revealed two dominant features: a strong peak centered at 351 nm that corresponds to the third harmonic of the pump beam and the nitrogen emission line at 337 nm. All other UV and visible nitrogen lines, both molecular and ionic, were too weak to be detected. Emission in both detectable spectral features was linearly polarized parallel to the polarization direction of the pump light at 1053 nm. This suggests that the nitrogen emission at 337 nm was seeded by the short-wavelength spectral tail of the third harmonic of the pump.

An example of the recorded UV part of spectrum is shown in Fig. 2. In this measurement, the pump pulse energy and duration were 10 J and 10 ps, respectively, and an interference filter with a bandwidth of 10 nm and center wavelength of 340 nm was used. The intensity transmission curve for the filter is shown in the figure with a dashed line.

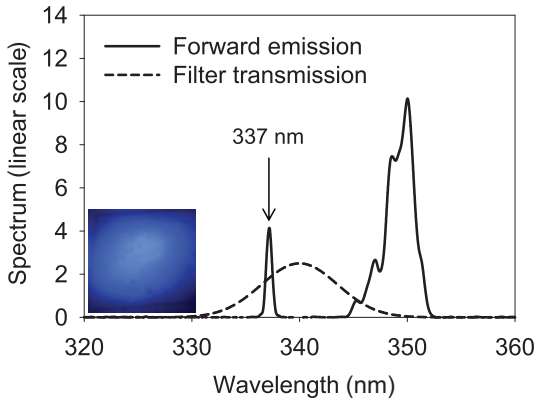

FIG. 2. (Color online) Spectrum of the forward-propagating UV optical signal. The inset shows the photograph of the far-field intensity distribution of the third harmonic of the pump beam with angular divergence of about 1.5°.

The photograph of the fluorescence induced by the third harmonic beam on a paper screen is shown in the inset in Fig. 2. The far-field divergence angle of the beam is about 1.5°. By translating the spectrometer slit across the beam and recording the amplitude of the 337-nm line as a function of the transverse displacement, we found that the divergence of the 337-nm beam was also about 1.5°.

For pulse energy characterization, the forward-propagating UV beam was collected with a 75-mm-diam fused silica lens and its energy was measured with a pyroelectric sensor. Appropriate combinations of interference UV filters were used to isolate the 351-nm (third harmonic of the pump) and 337-nm spectral lines. In Fig. 3 we show the energy of the 337-nm pulse as a function of the full width at half maximum duration of the pump pulse. When taking this data, the duration of the pump pulse and its energy were varied together so that the peak pulse power was kept at 1 TW. The maximum measured energy in the 337-nm pulse is about 2.5 μJ. It is obtained at the longest pump pulse used, which, at a fixed peak power of the pump pulse, corresponds to the highest pump energy of 10 J. The estimated corresponding conversion efficiency from the 1053-nm pump into the 337-nm emission is 2.5×10^{-7}. At that point, the

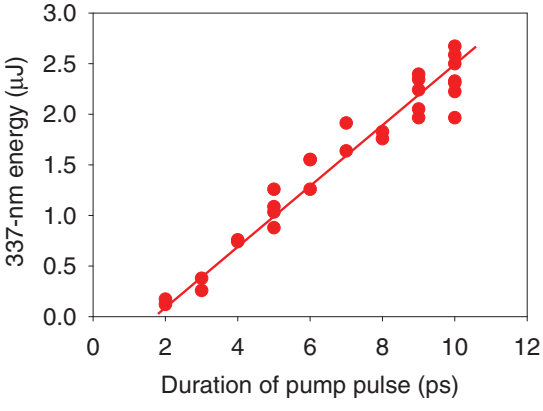

FIG. 3. (Color online) Energy in the forward-propagating 337-nm spectral line as a function of the full width at half maximum duration of the pump pulse. The peak power of the pump pulse is kept constant at 1 TW.

measured energy in the third harmonic of the pump was 700 μJ, corresponding to a conversion efficiency of 7×10^{-5}.

Attempts to measure any UV emission in the backward direction, using a 45° dichroic pellicle beam splitter placed after the meniscus lens, were not successful. We estimate that the backward-propagating emission at 337-nm wavelength, if generated above the spontaneous-emission level, was by at least two orders of magnitude weaker than the forward-propagating 337-nm pulse. This is not surprising, as both the traveling-wave mode of excitation and the seeding of the 337-nm gain by the third harmonic of the pump pulse make the generation in the forward direction favorable. Possible ways of eliminating the seeding are through the use of a circularly polarized pump pulse or by pumping at a wavelength that has no odd harmonics in the spectral vicinity of the 337-nm transition of nitrogen. It has been shown that with no external seeding applied, bidirectional operation of an amplified spontaneous emission laser is possible under traveling-wave excitation [3,14].

Rigorous analytical description of our experiment would require a model that treats the propagation of the pump field, its third harmonic, and the generated amplified spontaneous emission field, as well as the temporally and spatially resolved medium response, in a self-consistent manner. The development of such a comprehensive model is a formidable task that is beyond the scope of this Rapid Communication. In order to gain a qualitative insight into the physics of the generation of the forward-propagating 337-nm pulse in our setup, we numerically investigated the medium response, assuming a particular time dependence of pump intensity in the interaction zone that was derived from physical arguments as follows.

As the focused pump beam propagates towards the interaction zone, its intensity builds up due to the relatively sharp focusing by the meniscus lens with the f-number $N \approx 30$. The surge of intensity is eventually limited by the onset of plasma refraction, similar to the situation in femtosecond laser filaments [15]. The density of plasma that is necessary for the compensation of the beam focusing can be estimated as $n^* \approx n_c/4N^2$, where n_c is the critical plasma density, at which plasma becomes opaque for the pump light at 1053-nm wavelength. For our experimental geometry, $n^* \approx 3 \times 10^{17}/\mathrm{cm}^3$, which corresponds to ionization of about 1% of all neutral molecules of air. Considering a 10-J, ~10-ps-long pump pulse and noting that the propagation of its leading temporal edge is governed by the lens focusing only, we find that such a level of ionization is reached within the first few hundred femtoseconds of the temporal pulse envelope, via photoionization with the rate calculated according to the Perelomov-Popov-Terent'ev model [16]. As the calculation shows, at the point of time when plasma density reaches n^*, the optical intensity is about 7×10^{13} W/cm^2. If the intensity was kept clamped at that level throughout the remaining duration of the pulse, an optically driven avalanche would cause the gas to be completely ionized, which is unphysical. In reality, the surge of ionization will be prevented through the continuing transverse expansion of the focal zone driven by plasma refraction. The on-axis intensity will be correspondingly tapered off so that the plasma density will remain at a level not significantly exceeding n^*, just where it needs to be in order to compensate for the lens focusing. We approximate the intensity decay, from the point in time when

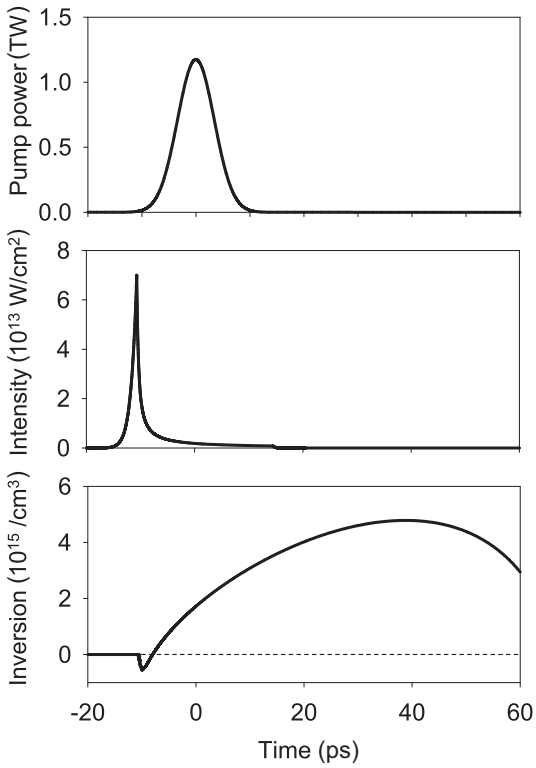

FIG. 4. Modeling results for the case of pumping with a 10-J 8-ps pulse. The top plot shows the time-dependent power of the pump pulse, the middle the intensity of the pump field in the interaction zone, and the bottom the time dependence of the population inversion on the 337-nm transition of nitrogen.

the plasma density reaches n^* and on, by a decaying function such that the instantaneous rate of that decay is proportional to the rate of the electron density growth and the resulting plasma density never exceeds n^* by 30%. The time-dependent intensity in the interaction zone, constructed based on the above logic, is shown in the middle part of Fig. 4 for the case of a 10-J 8-ps-long pump pulse. The time-dependent pulse power is shown in the top part of the figure. Throughout the major part of the pulse duration, the intensity is between 1.5 and 5×10^{12} W/cm^2. These values are consistent with the TW-level peak power of the pump pulse being spread over the beam with a diameter of ~5 mm, which was experimentally found from the burn pattern produced by the focused beam on a glass surface.

Having had constructed the time dependence of the optical intensity in the interaction zone, we compute the medium response in this field by solving the Boltzmann equation in the Lorenz approximation for the electron energy distribution function (EEDF) [17]. The Boltzmann equation for the EEDF is coupled to the set of rate equations for the populations of different electronic states of nitrogen molecules. Our model accounts for elastic collisions of electrons with nitrogen and oxygen molecules; inverse bremsstrahlung heating; inelastic collisions with nitrogen molecules resulting in excitation and deexcitation of states $A\,^3\Sigma_u$, $B\,^3\pi_g$, $a\,^1\Sigma_u$, $a\,^1\pi_g$, and $C\,^3\pi_u$; superelastic collisions; vibrational excitation of nitrogen and oxygen; electron-electron Coulomb scattering [18]; electron impact ionization; and electron-molecular ion recombination. The corresponding electron energy-dependent cross sections

for the above processes are taken from [19–21]. The rate equations account for collisional quenching of the excited states of nitrogen with reaction constants from [13]. The effects of the generated amplified spontaneous emission field at 337 nm on the medium are neglected.

Excitation of neutral nitrogen molecules by electron impact is an established mechanism for the development of population inversion in conventional UV nitrogen lasers pumped by electrical discharge. Similar to those conventional nitrogen lasers, in our case, which involves pumping by a picosecond laser source, hot electrons are generated that are capable of inverting the 337-nm transition on impact with neutral nitrogen molecules. Accordingly, we assume that the dominant mechanism for the creation of population inversion in our case is through electron impact excitation. Additional mechanisms contributing to the population inversion may be operative, e.g., the channel that involves the formation of the cluster ion N_4^+, as suggested in [22,23]. In our model that excitation channel is assumed to be dominated by electron impact excitation.

An example of the application of our model is shown in the bottom part of Fig. 4. The temporal evolution of the population inversion density on the 337-nm transition between the $C\,^3\pi_u$ and $B\,^3\pi_g$ states of nitrogen molecule is calculated for the case of pumping with a 10-J 8-ps-long pulse at 1053 nm. As evident from this simulation, the population inversion is negative through the approximately 2.5-ps-long time window at the very beginning of the pulse, but then changes sign and remains positive for tens of picoseconds. Through the beginning of the pulse, the generated electrons become sufficiently heated by the laser field so that they start predominantly exciting the upper energy state responsible for the 337-nm emission. For pump pulses that are longer than 2.5 ps, the pump pulse (and its third harmonic) are still present when the population inversion becomes positive. In that case, the third harmonic of the pump is available to seed the 337-nm emission through the remaining part of the pulse. For pump pulses shorter than 2.5 ps, population inversion may still develop on the 337-nm transition under some conditions, but by the time it develops the third harmonic of the pump is gone and not available to seed the inversion. The outcome of the model is in qualitative agreement with our experimental results that show a threshold for the appearance of the 337-nm emission with respect to the duration of the pump pulse.

The authors acknowledge helpful discussions with Audrius Pugžlys, Luc Berge, Howard Milchberg, and Mikhail Shneider. This work was supported by the United States Air Force Office of Scientific Research under Programs No. FA9550-12-1-0143, No. FA9550-12-1-0482, and No. FA9550-10-1-0561 and by the European Union under the CROSS TRAP project. A.S.-S. acknowledges the support from the US NRC postdoctoral fellowship. The use of the Jupiter Laser Facility was supported by the US Department of Energy, Lawrence Livermore National Laboratory, under Contract No. DE-AC52-07NA27344.

[1] P. R. Hemmer, R. B. Miles, P. Polynkin, T. Siebert, A. V. Sokolov, P. Sprangle, and M. O. Scully, Proc. Natl. Acad. Sci. USA **108**, 3130 (2011).

[2] L. Yuan, A. A. Lanin, P. K. Jha, A. J. Traverso, D. V. Voronine, K. E. Dorfman, A. B. Fedotov, G. R. Welch, A. V. Sokolov, A. M. Zheltikov, and M. O. Scully, Laser Phys. Lett. **8**, 736 (2011).

[3] A. Dogariu, J. Michael, M. O. Scully, and R. Miles, Science **331**, 442 (2011).

[4] A. J. Traverso, R. Sanchez-Gonzalez, L. Yuan, K. Wang, D. V. Voronine, A. M. Zheltikov, Y. Rostovtsev, V. A. Sautenkov, A. V. Sokolov, S. W. North, and M. O. Scully, Proc. Natl. Acad. Sci. USA **109**, 15185 (2012).

[5] A. Couairon and A. Mysyrowicz, Phys. Rep. **441**, 47 (2007).

[6] L. Berge, S. Skupin, R. Nuter, J. Kasparian, and J.-P. Wolf, Rep. Prog. Phys. **70**, 1633 (2007).

[7] S. L. Chin, *Femtosecond Laser Filamentation* (Springer, New York, 2010).

[8] Q. Lou, W. Liu, and S. L. Chin, Appl. Phys. B **76**, 337 (2003).

[9] J. Yao, B. Zeng, H. Xu, G. Li, W. Chu, J. Ni, H. Zhang, S. L. Chin, Y. Cheng, and Z. Xu, Phys. Rev. A **84**, 051802(R) (2011).

[10] J. Ni, W. Chu, H. Zhang, C. Jing, J. Yao, H. Xu, B. Zeng, G. Li, C. Zhang, S. L. Chin, Y. Cheng, and Z. Xu, Opt. Express **20**, 20970 (2012).

[11] V. A. Vaulin, V. N. Slinko, and S. S. Sulakshin, Kvantovaya Elektron. (Moscow) **15**, 2329 (1988) [Sov. J. Quantum Electron. **18**, 1457 (1988)].

[12] https://jlf.llnl.gov.

[13] I. A. Kossyi, A. Yu. Kostinsky, A. A. Matveyev, and V. P. Silakov, Plasma Source Sci. Technol. **1**, 207 (1992).

[14] G. J. Pert, Opt. Commun. **191**, 113 (2001).

[15] S. Xu, J. Bernhardt, M. Sarifi, W. Liu, and S. L. Chin, Laser Phys. **22**, 195 (2012).

[16] A. M. Perelomov, V. S. Popov, and M. V. Terent'ev, Zh. Eksp. Teor. Fiz. **50**, 1393 (1966) [Sov. Phys. JETP **23**, 924 (1966)].

[17] Yu. P. Raizer, *Gas Discharge Physics* (Springer, Berlin, 1991).

[18] S. Rockwood, Phys. Rev. A **8**, 2348 (1973).

[19] Y. Itikawa, J. Phys. Chem. Ref. Data **35**, 31 (2006).

[20] Y. Itikawa, J. Phys. Chem. Ref. Data **38**, 1 (2009).

[21] J. Bacri and A. Medani, Physica B + C **112**, 101 (1982).

[22] H. L. Xu, A. Azarm, J. Bernhardt, Y. Kamali, and S. L. Chin, Chem. Phys. **360**, 171 (2009).

[23] J. Peñano, P. Sprangle, B. Hafizi, D. Gordon, R. Fernsler, and M. Scully, J. Appl. Phys. **111**, 033105 (2012).